# Electronic Supplementary Information

## Enhancing Cu-Ligand Interaction for Efficient $CO_2$ Reduction towards Multi-carbon Products

Jingyi Chen[+ [a]], Lei Fan[+ [a]], Yilin Zhao[a], Haozhou Yang[a], Di Wang[a], Bihao Hu[a], Shibo Xi[b], and Lei Wang*[a,c]

[a] Department of Chemical and Biomolecular Engineering, National University of Singapore, 4 Engineering Drive 4, Singapore 117585

[b] Institute of Sustainability for Chemicals, Energy and Environment, A*STAR, 1 Pesek Road, Jurong Island, Singapore 627833

[c] Centre for Hydrogen Innovations, National University of Singapore, 4 Engineering Drive 4, Singapore 117585

[+] These authors contributed equally to this work.

E-mail: wanglei8@nus.edu.sg

**Table of content**

**Experimental Procedures**

**Chemicals and materials:** Copper(II) sulfate ($CuSO_4$, 99%), 3,5-Diamino-1,2,4-triazole ($C_2H_5N_5$, 98%), 3-Amino-1,2,4-triazole ($C_2H_4N_4$, 95%), 1,2,4-Triazole ($C_2H_3N_3$, 98%), Copper nanopowder (60-80 nm, 99.5%), Potassium bicarbonate ($KHCO_3$, 99.999%) were purchased from Sigma-Aldrich. All reagents were used as received without further purification.

**Material characterizations:** Transmission electron microscopy (TEM) and corresponding energy-dispersive X-ray spectroscopy (EDS) were taken by a JEOL JEM-2010F TEM. Scanning electron microscope (SEM) and corresponding energy-dispersive X-ray spectroscopy (EDS) were carried by JEOL JSM-7610F SEM. X-ray photoelectron spectroscopy (XPS) was conducted on Kratos Axis UltraDLD (Mono Al Kα, hν= 1486.71 eV). Fourier-transform infrared spectroscopy (FTIR) was recorded using VERTEX 70 FT-IR Spectrometer. In-situ FTIR was measured by Shimadzu IR tracer-100 FTIR Spectrophotometer. XAS was performed at XAFCA beamline of Singapore Synchrotron Light Source under transmission mode. Cu K-edge XANES and EXAFS spectra were collected. And data process was processed by Athena.

**Synthesis of Cu(II) complexes**: For CuDAT, 2 mmol $Cu(SO_4)\cdot 5H_2O$ is dissolved in 10 mL deionized water. Then, 10 mL water solution of 3,5-Diamino-1,2,4-triazole (4 mmol) is dropped $Cu(SO_4)\cdot 5H_2O$ solution under vigorous stirring. After stirring for 4 hours, the products were collected *via* centrifuge at 5000 rpm for 5 minutes and washed three times with deionized water. The resulting samples were dried in vacuum at room temperature overnight. For CuAT and CuT synthesizing, 3-Amino-1,2,4-triazole ($C_2H_4N_4$, 95%) and 1,2,4-Triazole were applied as the ligand, following the same procedure as CuDAT synthesis.

**$CO_2R$ measurements in the flow cell:** 4 mg samples (CuDAT, CuAT, CuT and CuNPs) were dispersed in the mixed solution containing 400 uL ethanol and 16 uL 5 wt% Nafion. The ink was sonicated for 30 min and sprayed on carbon paper (1.2*1.2 $cm^2$, Fuel Cell Gas Diffusion Layer YLS30T) to reach the loading of 1 mg $cm^{-2}$. The reaction was conducted in a self-designed flow cell with a catalyst area of 1 $cm^2$. The prepared carbon paper was used as the working electrode, while Ag/AgCl electrode and Pt foil were used as the reference electrode and counter electrode, respectively. All the recorded potentials were converted to RHE scale based on:

$$E\ (\text{vs. RHE}) = E\ (\text{vs. Ag/AgCl}) + 0.197\ \text{V} + 0.0591\ \text{V} \times \text{pH} - I \times R_s$$

Anion exchange membrane (Selemion AMN/N type 1, AGG Inc.) was applied to separate two compartments. Bio-Logic VMP3 multichannel potentiostat was used for controlling electrochemical measurement. During $CO_2$ reduction, $CO_2$ was flowed continuously through the gas chamber at a rate of 20 sccm. The catholyte (1 M $KHCO_3$) and anolyte (1 M KOH) flowed at a rate of 10 mL/min under the control of a peristaltic pump. The gas products were analyzed by gas chromatography (GC, Shimadzu 2014). Liquid products were analyzed by $^1H$ NMR spectrum (Bruker, 400 MHz). Faradic efficiency (FE) for each product was calculated based on:

$$FE = \text{Product amount (mol)} \times \text{n} \times \text{F (C/mol)} \Big/ I\ (A) \times \text{t (s)}$$

where n is the electron transfer number of a specific product, F is the Faradic efficiency (96485 C/mol), I is the total current, and t is reaction time.

**Electrochemical surface area measurement:** The ECSA test was performed in a standard three-electrode system with CuDAT/CuNPs loaded carbon paper as the working electrode, Ag/AgCl as the reference electrode, and platinum foil as the counter electrode. CV tests at different scan rate (20, 40, 60, 80, 100, 120, 140, 160 mV/s) were carried in Ar-saturated 0.1 M $KHCO_3$. The normalized current density was calculated based on:

$$\text{ECSA normalized j} = I \Big/ S_{ECSA}$$

$$S_{ECSA} = C_{dl} \Big/ C_S$$

where I is current (mA), $C_{dl}$ is measured double layer capacitance of catalysts, and $C_s$ is $C_{dl}$ for planar polycrystalline Cu (= 29 μF).[1]

**In-situ ATR-SEIRAS:** The working electrode was prepared on Au film that was pre-deposited onto a silicon attenuated total reflection (ATR) crystal via chemical deposition. 5 mg catalyst (CuDAT or CuNPs) was dispersed in 500 uL ethanol and 20 uL 5 wt% Nafion solution to form a homogeneous ink by sonicating. Then, the ink was dropped onto the Au film. The prepared working electrode was assembled into an H cell. Ag/AgCl electrode and graphite rod served as reference and counter electrodes, respectively. Anion exchange membrane (Selemion AMN/N type 1, AGG Inc.) was applied to separate two compartments, 0.2 M $KHCO_3$ was used as both catholyte and anolyte with continuous $CO_2$ purging, and CHI760e potentiostat was employed to control overpotential. The H cell was assembled Shimadzu IR tracer-100 FTIR Spectrophotometer. Before data collecting, the background was recorded at open circuit potential. During the experiment, the overpotential changed from −0.4 V vs. RHE to −1.4 V vs. RHE. All data was presented in absorbance units.

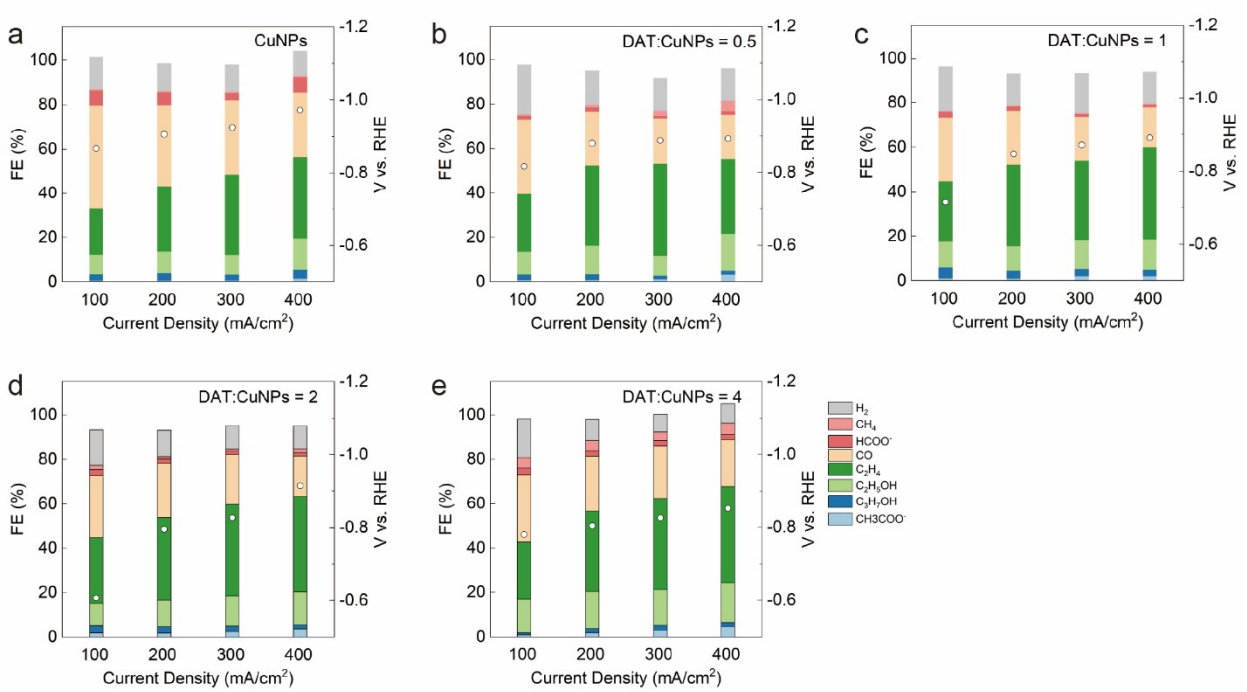


**Figure S1** $CO_2$ reduction performance of the physical mixture of DAT and CuNPs with molar ratio from 0 to 4 (a-e).

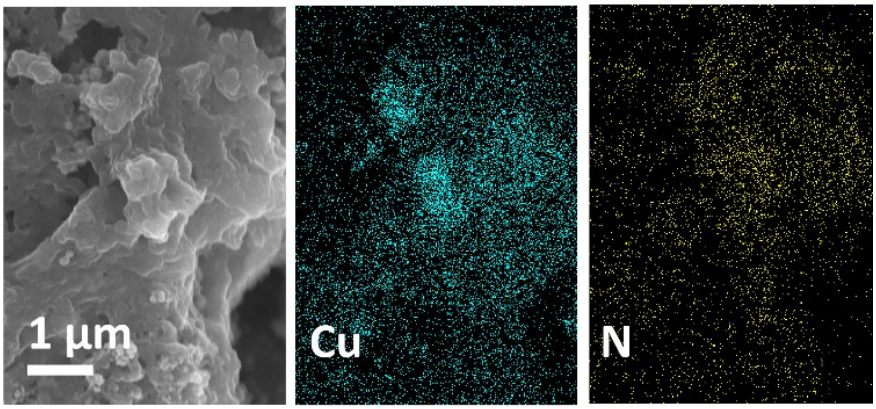


**Figure S2** EDS mapping of post-reaction mixture between CuNPs and DAT ligand.

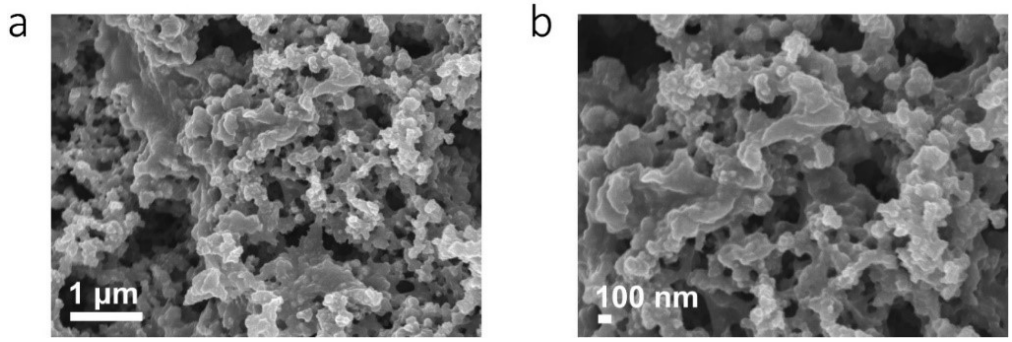


**Figure S3** SEM image for post-reaction sample of CuNPs and DAT ligand mixture. Parts of Cu particles are exposed in the absence of ligand modification.

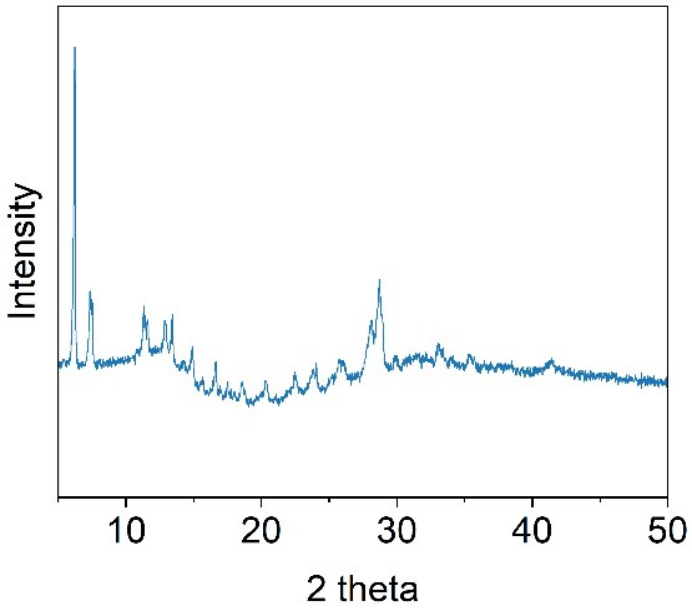


**Figure S4** XRD of as-prepared CuDAT.

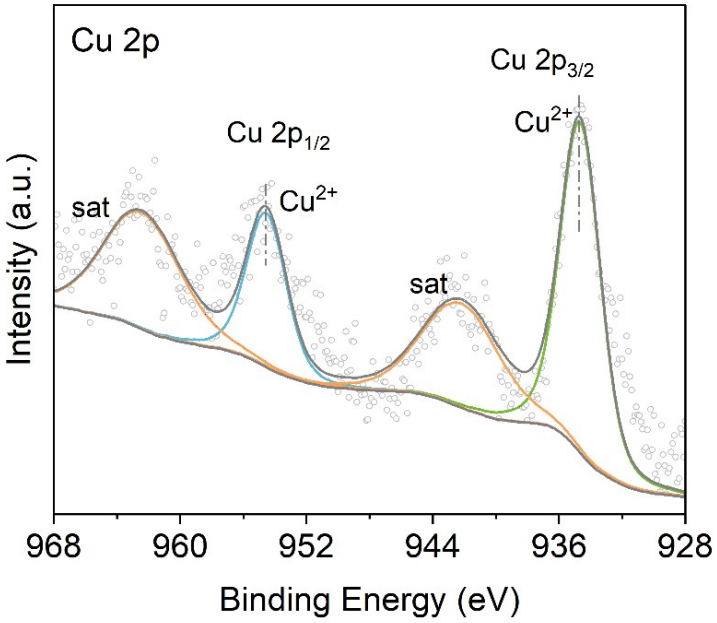


**Figure S5** Cu *2p* XPS of as-prepared CuDAT sample.

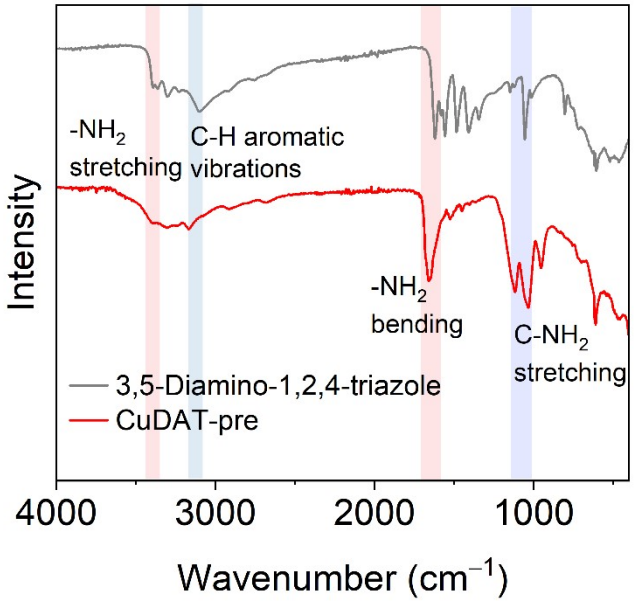


v

**Figure S6** ATR-FTIR spectrum of as-prepared CuDAT.

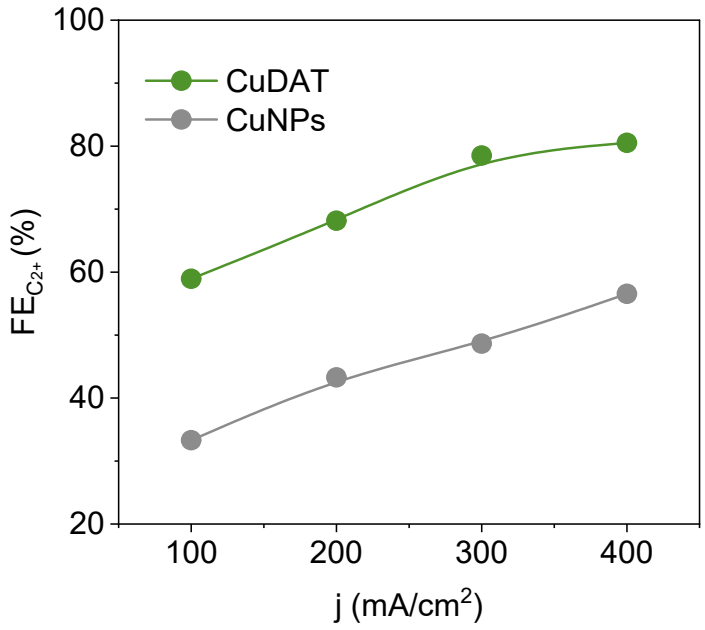


**Figure S7** FE($C_{2+}$) comparison of CuDAT and CuNPs at different current density.

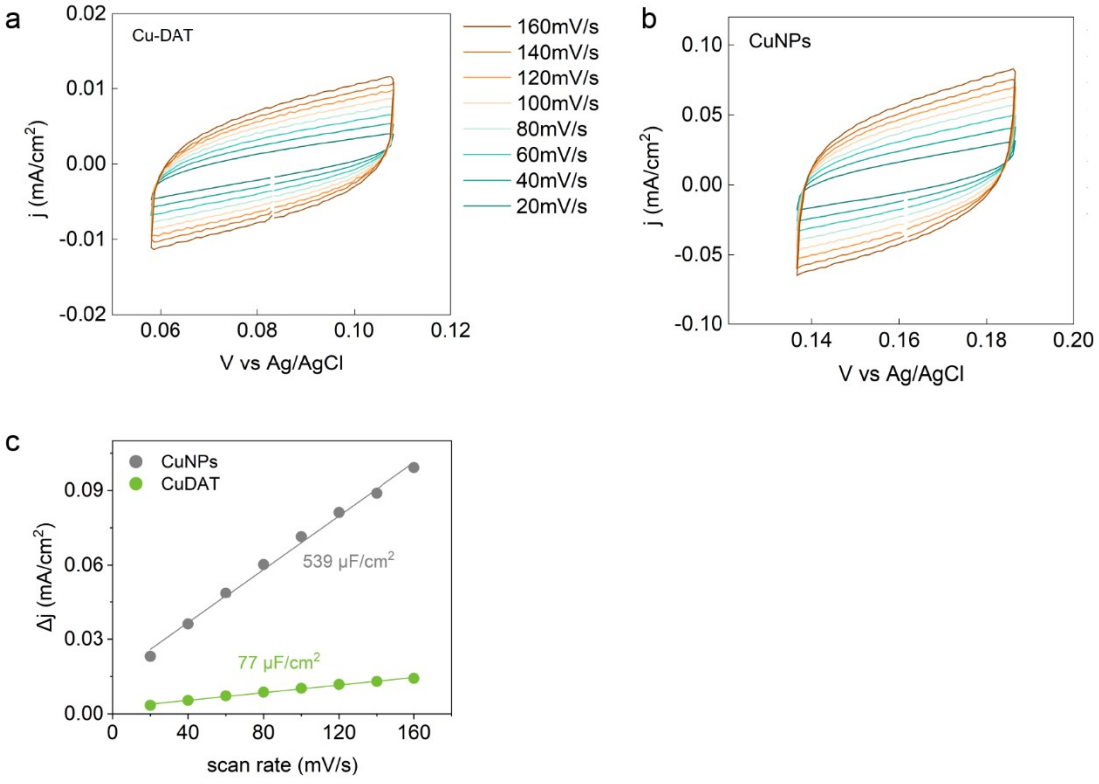


**Figure S8** The cyclic voltammetry curve of (a) CuDAT, (b) CuNPs in Ar-saturated 1M $KHCO_3$. (c)The fitted electrical double layer capacitance of CuDAT and CuNPs.

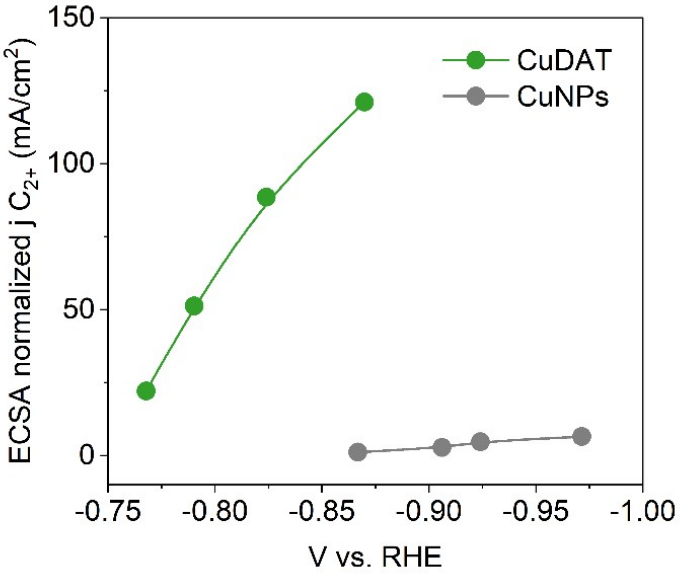


**Figure S9** ECSA normalized current density of CuDAT and CuNPs.

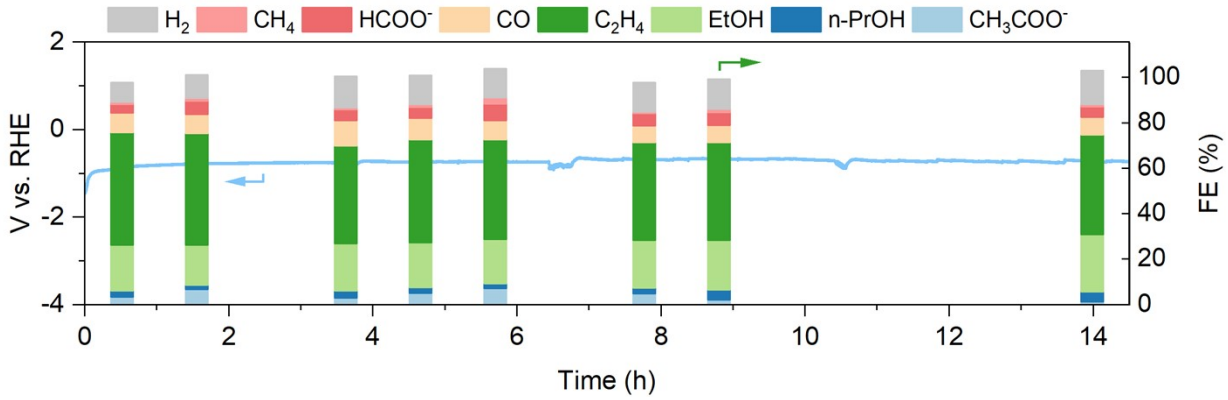


**Figure S10** $CO_2R$ stability test on CuDAT at 200 mA $cm^{-2}$.

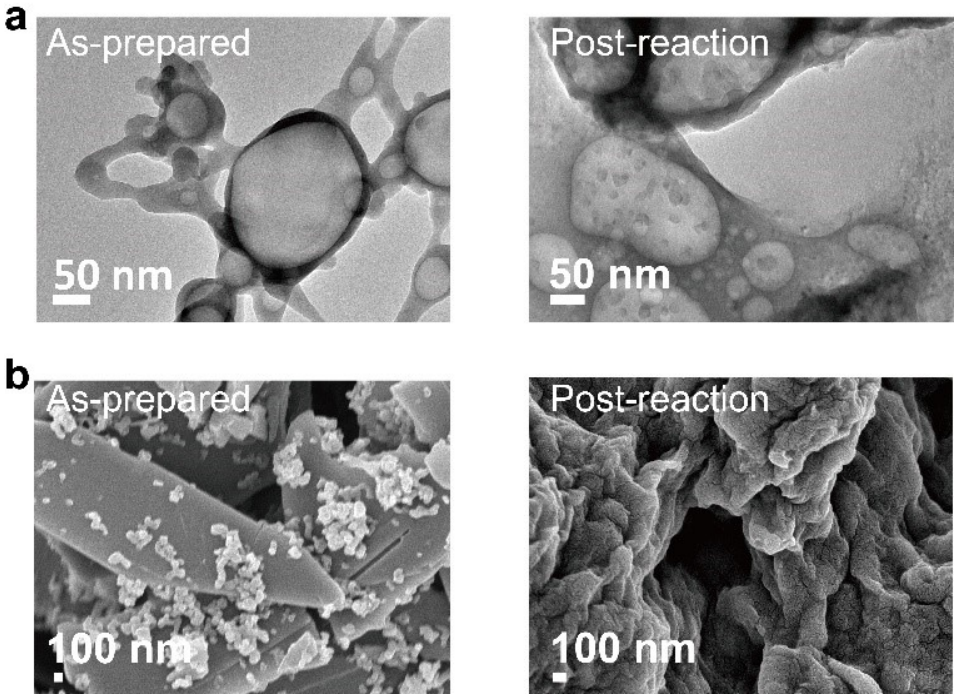


**Figure S11** (a) SEM and (b) TEM images of post-reaction CuDAT. (c) SEM images of as-prepared CuDAT.

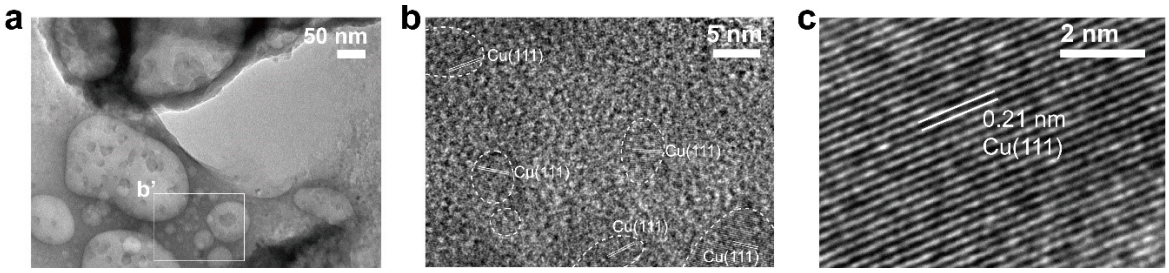


**Figure S12** (a) TEM image and (b, c) HRTEM images of post-reaction CuDAT samples. Zero-valance Cu aggregation happens with the particle size ~5 nm.

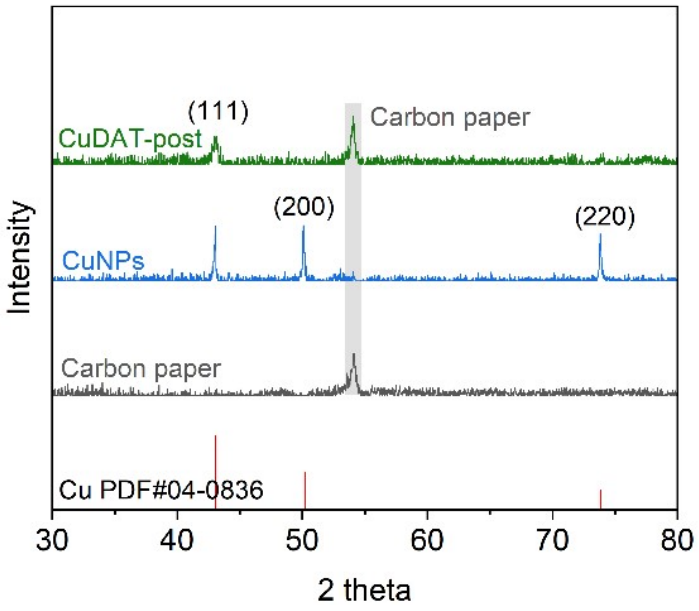


**Figure S13** XRD of post-reaction CuDAT, commercial CuNPs and carbon paper substrate.

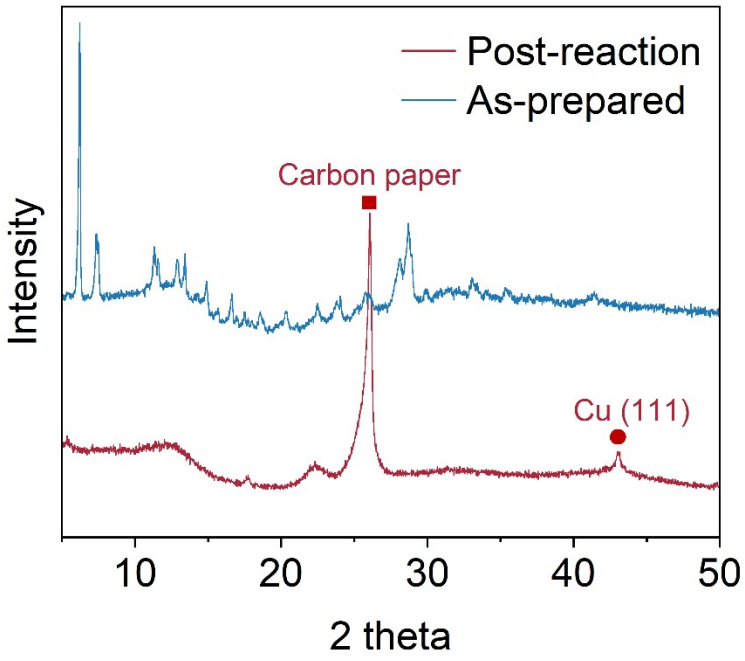


**Figure S14** XRD of as-prepared and post-reaction CuDAT.

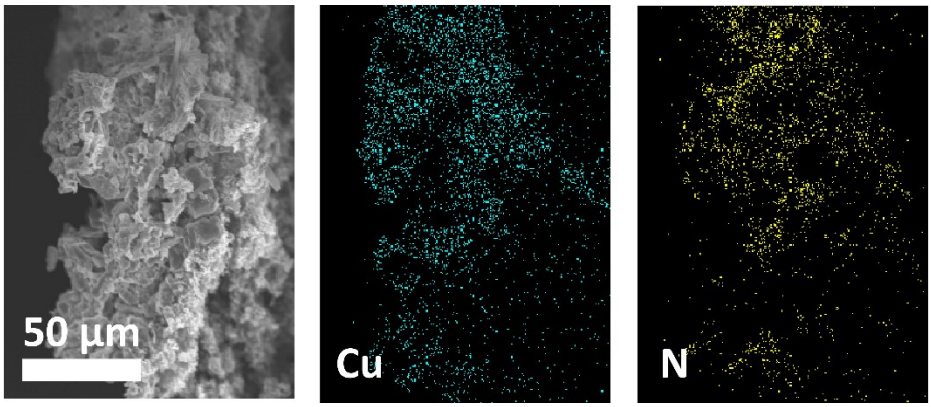


**Figure S15** Cross-section EDS mapping of post-reaction CuDAT.

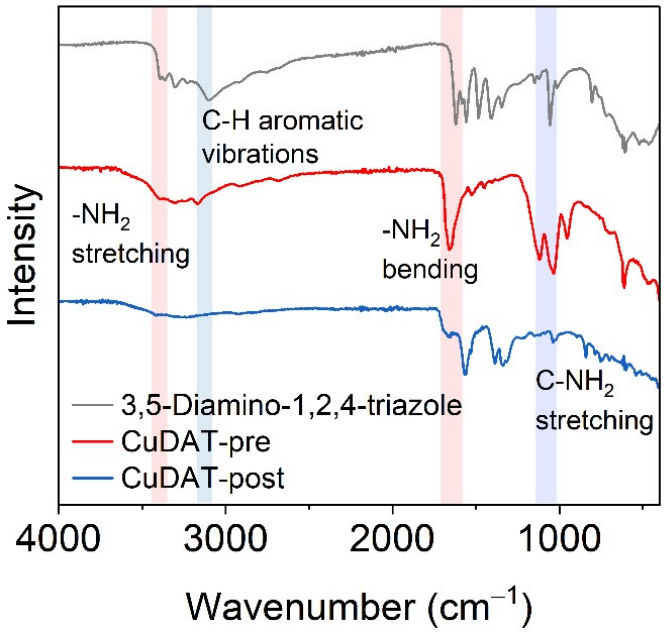


**Figure S16** ATR-FTIR spectra of post-reaction CuDAT.

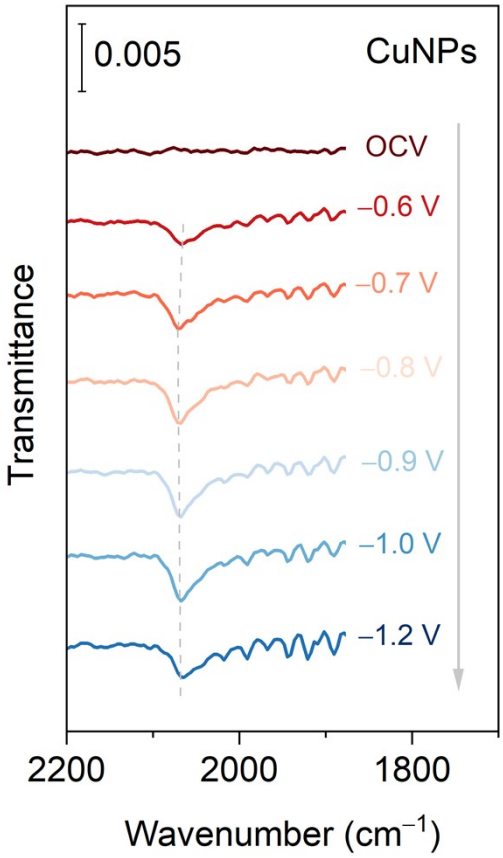


**Figure S17** *In situ*-ATR-SEIRAS spectra of commercial CuNPs.

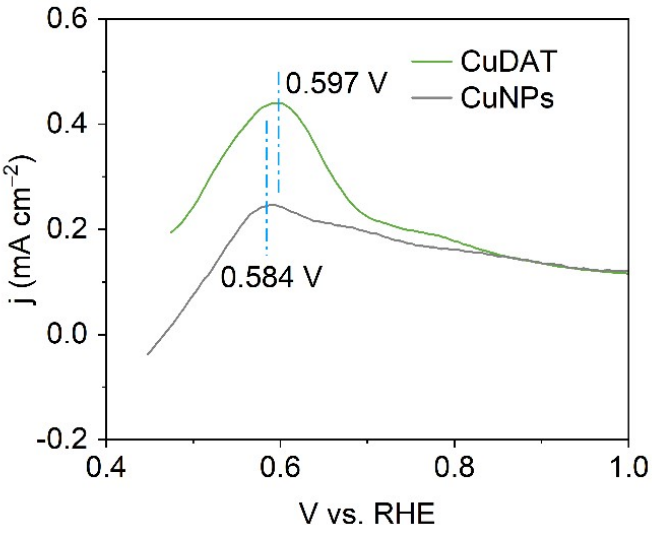


**Fig. S18** CO stripping on CuDAT and CuNPs with the scan rate of 10 mV S-1, after 10 s CO adsorption at -0.3 V in CO saturated 0.1 M KOH.

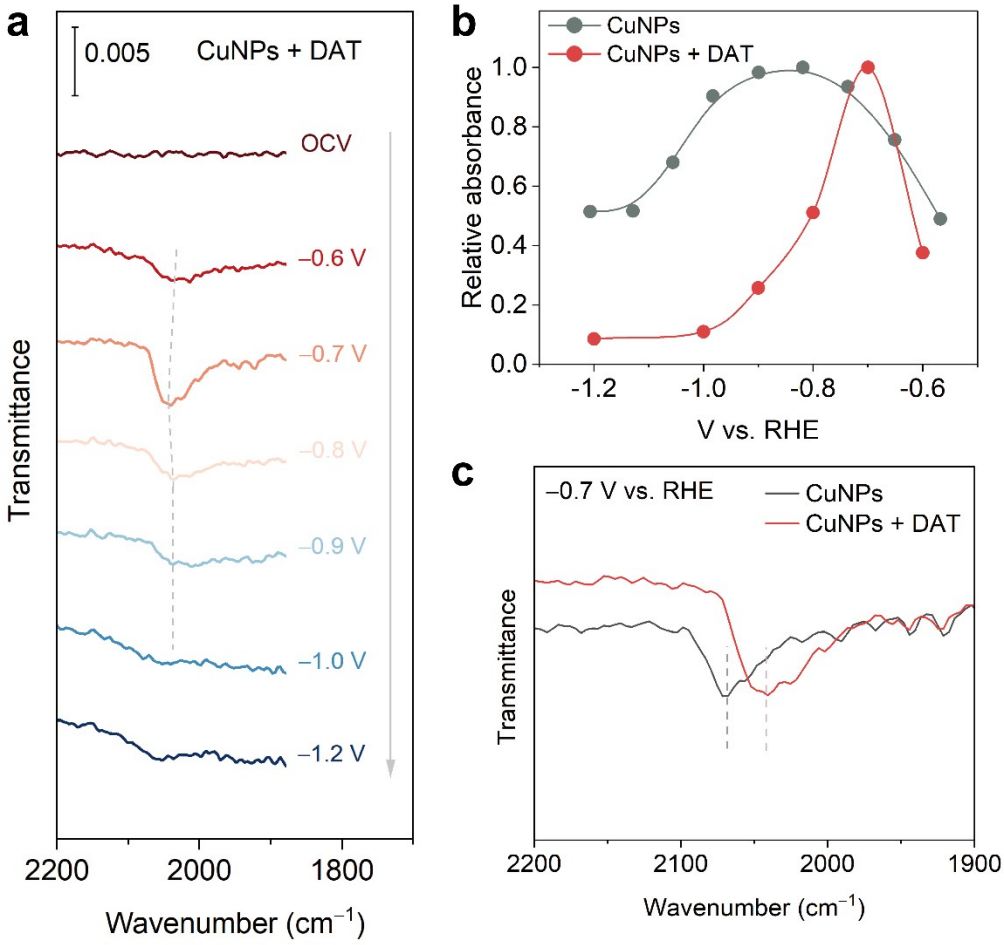


**Figure S19** (a) In-situ ATR-SEIRAS of physical mixture of commercial CuNPs and DAT ligand during $CO_2R$ (the mass ratio of DAT to CuNPs = 2). (b) Relative absorbance of $*CO_L$ band for CuNPs, and physical mixture of CuNPs and DAT ligand. (c) $*CO_L$ band in in-situ ATR-SEIRAS of CuNPs, and physical mixture of CuNPs and DAT ligand, at –0.7 V vs. RHE.

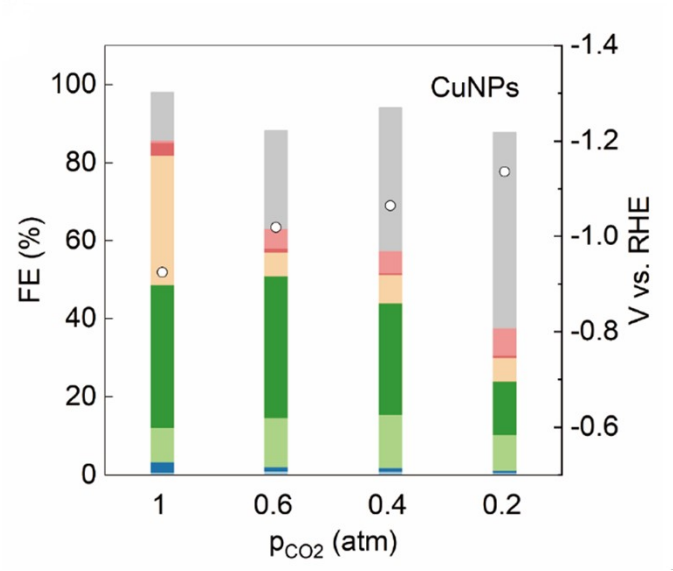


**Figure S20** Low-concentration $CO_2$ reduction performance of CuNPs in 1 M $KHCO_3$ at 300 mA $cm^{-2}$.

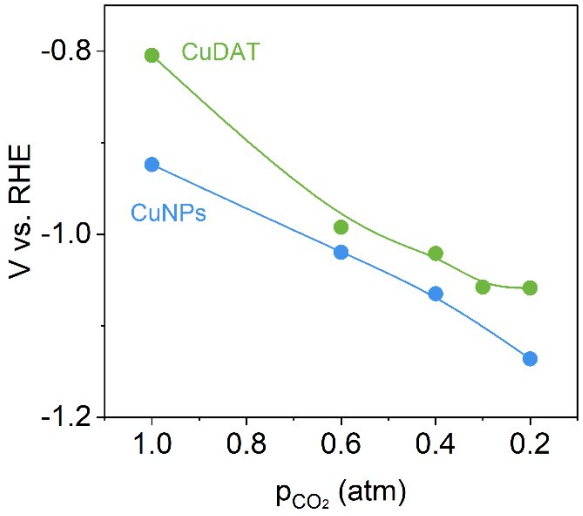


**Figure S21** Overpotential of CuDAT and CuNPs to achieve 300 mA $cm^{-2}$ at different CO2 partial pressure.

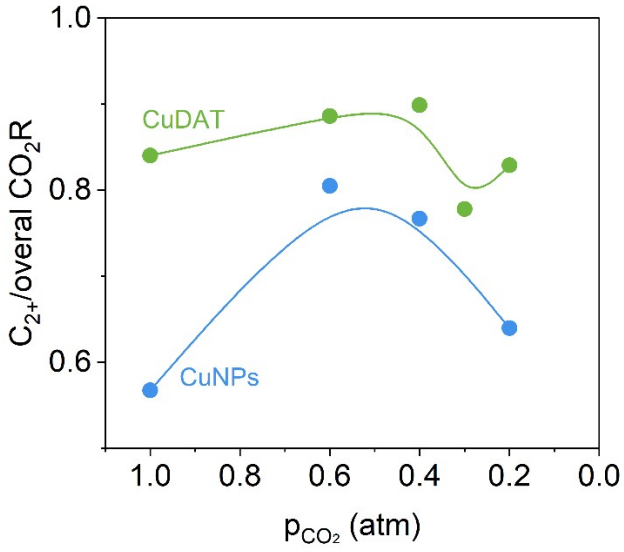


**Figure S22** FE($C_{2+}$)/FE($CO_2R$) for CuDAT and CuNPs with different p($CO_2$) at 300 mA $cm^{-2}$.

## Reference

(1) Wang, L.; Nitopi, S.; Wong, A. B.; Snider, J. L.; Nielander, A. C.; Morales-Guio, C. G.; Orazov, M.; Higgins, D. C.; Hahn, C.; Jaramillo, T. F. Electrochemically converting carbon monoxide to liquid fuels by directing selectivity with electrode surface area. *Nat. Catal.* **2019**, *2*, 702-708.